Journal of
Water & Climate Change

IWA PUBLISHING

Journal of Water and Climate Change Vol 00 No 0, 1 doi: 10.2166/wcc.2026.493

Assessment of social vulnerability under climate change risks in the southwestern coastal region of Bangladesh

Md. Kamrul Hasan [a,*], Md. Mizanur Rahman [b] and Abu Nayem Md. Kayes [a]

[a] Department of Urban and Regional Planning, Pabna University of Science & Technology, Pabna, Bangladesh
[b] Department of Geography and Environment, Jahangirnagar University, Savar, Dhaka, Bangladesh
*Corresponding author. E-mail: kamrul.urp@pust.ac.bd

MKH, 0000-0002-4404-9215; MMR, 0000-0001-5480-6315; ANMK, 0009-0002-0258-8859

ABSTRACT

Cyclones, storm surges, sea-level rise, tidal flooding, and limited adaptive capacity due to high population pressure and flat terrain make coastal Bangladesh highly vulnerable. This study assesses long-term climatic variability and household-level social vulnerability (SV) in Dacope Upazila, Khulna District, Bangladesh. Primary data were collected through semistructured household surveys using random sampling, while secondary climate data (1981–2021) were obtained from the NASA POWER database. The Mann–Kendall test was applied to evaluate the statistical significance of trends in rainfall and temperature, and Sen's slope method was used to estimate trend magnitude. Results indicate a downward trend in precipitation for January and February, with Z values of −0.096 and −0.042, respectively. Annual temperature also shows a decreasing trend ($Z = -0.422$). The rainfall anomaly index reveals that since 2015, values exceeding 1.3 indicate annual precipitation shifted from dry to extremely humid conditions. Future projections using global climate models suggest that maximum temperature may increase by 1–2 °C. SV was assessed using principal component analysis based on 28 indicators. The SV index score (+9.772) indicates high societal sensitivity to climate change. These findings can support policymakers in developing effective climate adaptation and disaster risk reduction strategies.

Key words: climate change, climatic trend analysis, coastal area, principal component analysis, social vulnerability, social vulnerability index

HIGHLIGHTS

- Introduced statistical approaches like the Mann–Kendall test to identify change in climatic elements like precipitation and temperature.
- Assessed social vulnerability in Dacope Upazila using principal component analysis and calculated the social vulnerability index, where primary data were collected from a household survey.
- Extracted eight principal components for social vulnerability assessment.

GRAPHICAL ABSTRACT

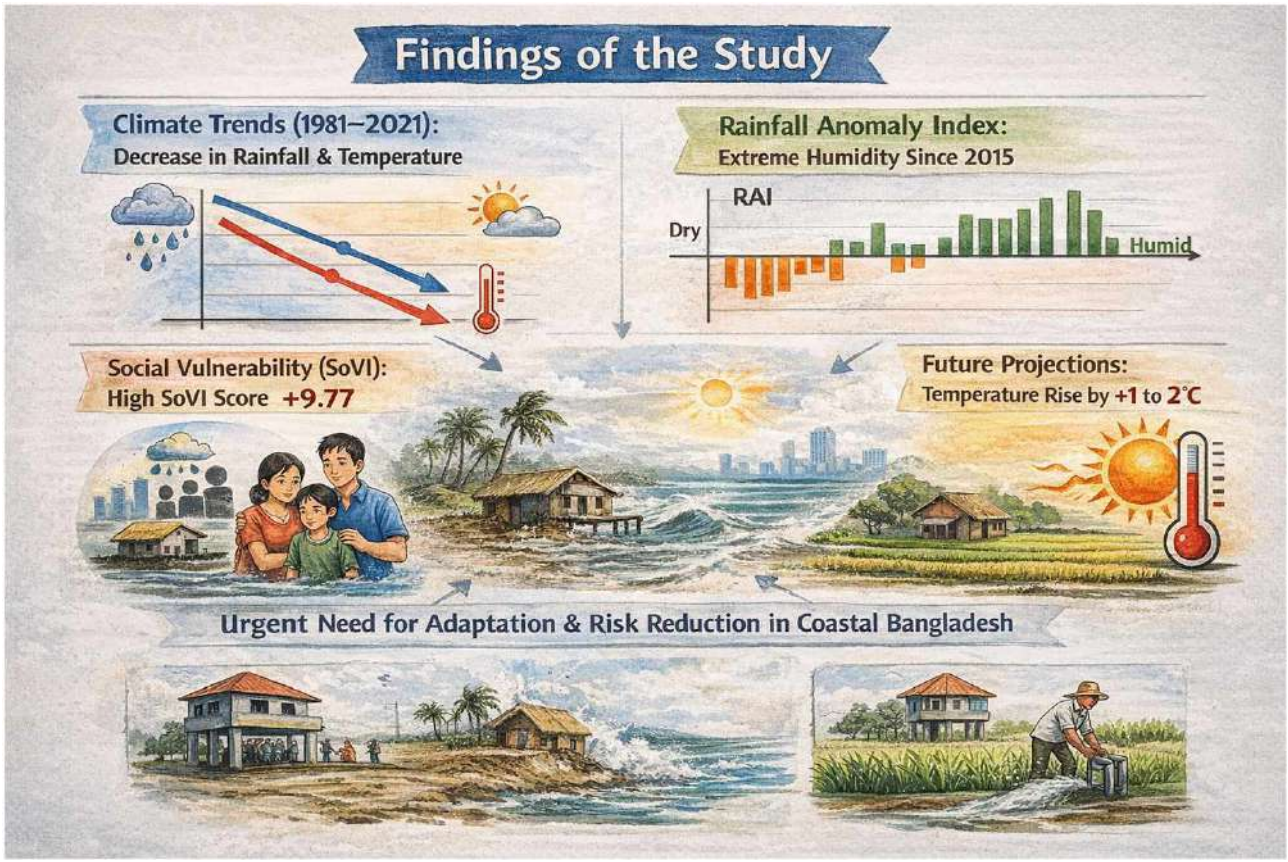

1. INTRODUCTION

Climate change represents a key global environmental challenge of the 21st century. Anthropogenic greenhouse gas emissions, chiefly from fossil fuel combustion and land use alterations, have led to elevated global temperatures, rising sea levels, and extreme weather phenomena (IPCC 2021). The Intergovernmental Panel on Climate Change (IPCC) cautions that unmitigated changes would result in devastating consequences for ecosystems, human health, and global economies (Cooper 2023). Developing countries, especially those with low-lying coastal regions, are disproportionately impacted by the detrimental effects of climate change owing to their restricted adaptive capacity and geographical susceptibility (Chowdhury *et al.* 2024b).

Bangladesh, as one of the most climate-vulnerable countries in the world, faces profound risks from climate change (Mojid 2020). It is situated at the confluence of the Ganges, Brahmaputra, and Meghna rivers, which makes it highly prone to flooding, storm surges, and rising sea levels (Huq & Ayers 2007). The Climate Risk Index, published annually by Germanwatch, consistently ranks Bangladesh among the top ten countries most affected by extreme weather events (Eckstein *et al.* 2020). As a result, climate change has become a pressing concern for policymakers, scientists, and development organizations in the country, focusing on both mitigation and adaptation strategies (Hasan *et al.* 2025c).

Due to its dense population, exposed infrastructure, and dependence on agricultural and fishing industries, Bangladesh is especially susceptible to the effects of climate change (Ahmed *et al.* 2019). Coastal communities, which are home to almost 32% of the population, are at increased risk of flooding, tidal surges, storms, and salt intrusion due to rising sea levels (Didar-Ul Islam *et al.* 2015). Tropical storms like cyclone Sidr in 2007, cyclone Aila in 2009, and cyclone Amphan in 2020 have become more common and stronger, which has led to a rise in their destructive potential, numerous casualties, and widespread economic and social upheaval in coastal areas (Alam & Collins 2010).

The majority of climate change effects in Bangladesh are expected to originate from the south, specifically the Bay of Bengal and the adjacent North Indian Ocean (Islam 2025). These ocean currents are the origins of tropical cyclones,

storm surges, coastal erosion, monsoon winds, evaporation for monsoon precipitation, floods, and salinity intrusion. Despite having such problems, existing literature is concentrated on adaptation, mitigation, and livelihood vulnerability. For example, Uddin (2023) explored migration due to climate change instead of considering migration a social issue. Moreover, they limited their work to a review rather than a quantitative approach. On the other hand, Hasan *et al.* (2025c) and Islam *et al.* (2019) worked on adaptation to climate change. Hasan *et al.* (2025c) gave an adaptation plan, and Islam *et al.* (2019) portrayed the vulnerable areas. Kayes *et al.* (2025a) conducted research on the coastal area of Bangladesh, specifically on Cox's Bazar district, and identified the livelihood vulnerability with adaptation strategies of the community engaged in the dry fish production industry. Another study by Islam (2025) on the impact of climate change on coastal areas found impacts on flooding, ecosystems, land, and so on.

Dacope Upazila, located in the Khulna District of southwestern Bangladesh, is one such region that has experienced the harsh consequences of climate change. Bordering the Sundarbans mangrove forest and the Bay of Bengal, Dacope is highly susceptible to cyclones, tidal flooding, and saltwater intrusion (Rahman *et al.* 2013). The region's reliance on agriculture and aquaculture, both of which are sensitive to climatic variations, further intensifies its vulnerability. Rising salinity levels have rendered vast tracts of agricultural land unproductive, forcing many farmers to abandon traditional rice cultivation in favor of shrimp farming, which in turn exacerbates the problem of salinization (Khan *et al.* 2011).

Therefore, there are gaps in existing literature that no research has been conducted on social vulnerability assessment using principal component analysis (PCA). Moreover, no studies have categorized the years into dry to extremely humid using the rainfall anomaly index (RAI) to assess the pattern of changing environment, mainly the Dacope Upazila of Bangladesh.

Based on the research gap, the following null hypothesis was drawn for this research:

- There is no significant difference in temperature and precipitation scenarios in Dacope Upazila.
- There is no impact of climate change on social vulnerability (SV).

The study tried to address three key research questions. The first question investigates whether temperature and precipitation levels have increased over the past decade. The second question examines the SV of the study area. Finally, if the area is found to be socially vulnerable, the study seeks to identify the primary factors contributing to this vulnerability. For policy making, planning, research allocation, and numerous other purposes, this research is necessary.

Considering the existing literature gaps and the significance of the topic, this research aims to assess and provide insights into climatic variability over the decades, as well as the SV of households in the study area. To achieve these goals, three specific objectives were established: the first is to analyze the variability of maximum temperature and precipitation in Dacope Upazila from 1981 to 2021; the second is to evaluate the SV of the study area; and the third is to predict future temperature trends.

2. MATERIALS AND METHODS

2.1. Study area

In the era of modern technology, where people are thriving and enjoying life with advanced innovations, Dacope stands as a stark contrast, telling a story of struggle, vulnerability, and loss, both of life and assets. The lives of the people in Dacope are filled with hardship and darkness, despite the area's natural beauty, with its rivers and oceans. Dacope is an Upazila (sub-district) among the nine Upazila of Khulna district. This area is surrounded by Batiaghata Upazila to the north, Batiaghata and Rampal Upazilas to the east, the Sundarbans to the south, and Paikgachha Upazila to the west. The study area covers 991.98 km^2, which is divided into nine unions and has a population of 159,362 (male population is 79,992 and female population is 79,370) (BBS 2023a). It is located 26 km away from Khulna District town. In this densely populated area, unlike other Upazilas, connectivity with Khulna main town is maintained solely through the Pasur and Pankhali rivers, relying on ferries due to the absence of a bridge. Only 25 km of road is pucca, 205 km is semipucca road, and, as a matter of concern, 657 km is katcha road (BBS 2023a). This situation underscores the challenges faced by the local population. More specifically, Dacope is located between 22°24′ and 22°40′ north latitudes and between 89°24′ and 89°35′ east longitudes (Figure 1). Rivers are spread like a net all over Dacope, adding a new degree of natural beauty and also a curse. The study area is located in the Ganges–Brahmaputra delta, one of the largest delta systems in the world. The region is characterized by low-lying topography, marshy land, numerous rivers, canals, and tidal floodplains. The rivers stand as witnesses to the discrimination between urbanization and neglect within the same geographical boundary. The main rivers in the area

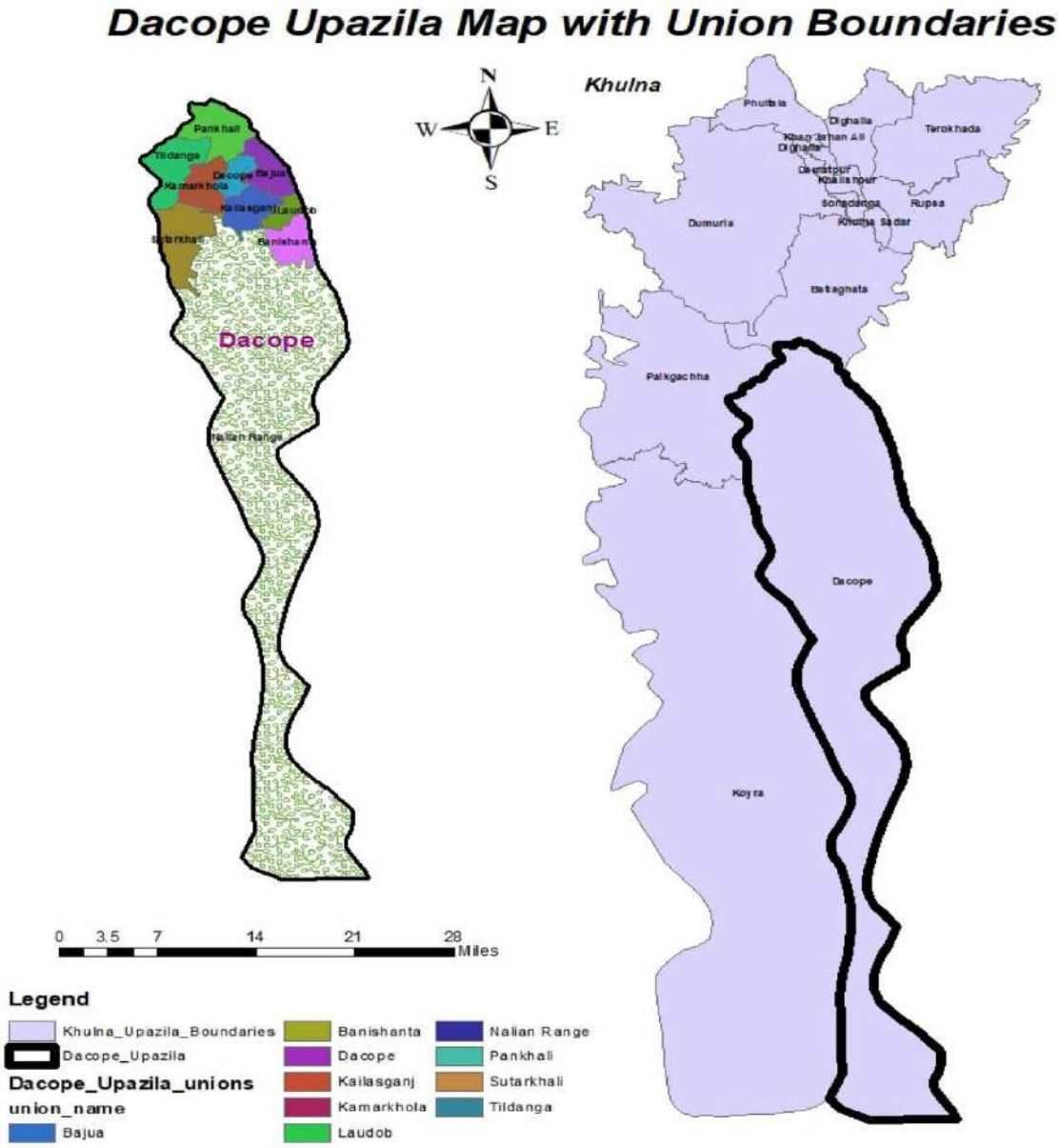

Figure 1 | Study area (Dacope Upazila, Khulna, Bangladesh). *Source*: Authors' illustration.

include Pasur, Shibsa, Manki, and Bhadra, with notable canals such as Palashbari, Churia, Nalian, and Jugra. The region is also home to the Sundarbans, the world's largest mangrove forest, which serves as a crucial source of fishing, honey collection, and raw materials for many households. Houses made of Golpata are common in Dacope Upazila. Cutting down the trees is also a concern of loss of biodiversity.

The biodiversity of Dacope Upazila is also rich due to the Sundarban. Some commonly found plants are Sundari, Golpata, Gewa, Keora, Goran, and so on. This coastal region has frequently suffered severe natural disasters, including river erosion and loss of life, over several decades. A network of 153 km of embankments was built in the 1960s to guard against erosion and floods. However, this initiative did not sustain effectiveness over the long term. In recent times, new embankments have been developed by the Water Development Board (WDB), often in collaboration with China. The quality of drinking water remains a critical concern in this region. Typically, the water in this region is saline, forcing residents to consume contaminated water. Subsequently, the Local Government Initiative on Climate Change (LoGIC) project, financed by the European

Union, Sweden, and Denmark, introduced a promising development: a water treatment facility established by the United Nations Development Programme (UNDP) in partnership with the government of Bangladesh and the United Nations Capital Development Fund (UNCDF).

The lives of the people are dependent on agriculture and fishing in this area. Agriculture, which generates 66.07% of Dacope Upazila's total revenue, is the major engine of the local economy (BBS 2023a). Nonetheless, the region's agricultural environment has seen a substantial change as saltwater prawn farming has become a prominent economic sector.

2.2. Data collection

There are mainly two types of data: (i) primary data (Section 2.2.2) and (ii) secondary data (Section 2.2.1), which were collected for conducting the study.

2.2.1. Climatic data

The essential main materials, comprising temperature and precipitation data, of the research area were obtained from (POWER | Data Access Viewer, NASA) and analyzed to discern the temperature trend over the 40 years (1981–2021) and precipitation over the identical 40-year span (1981–2021). NASA POWER products and observed data for all parameters are reliable, and the accuracy is good in humid regions. We primarily examined annual and seasonal patterns of temperature and precipitation (Tayyeh & Mohammed 2023).

The NASA POWER (Prediction of Worldwide Energy Resource) climate data, widely used for climate analysis, is subject to biases and limitations due to its modeling assumptions, satellite data calibration, and temporal resolution. These biases can arise from the mathematical models used for global reanalysis, which may not accurately represent local climate dynamics, especially in regions with complex topography and coastal influences. Additionally, the satellite data integrated into NASA POWER may suffer from calibration errors due to cloud cover and sensor limitations (NASA 2023). The spatial resolution of the dataset, at 0.5° × 0.5° (approximately 50 km), may not capture small-scale local climatic features or adequately represent heterogeneous landscapes, such as coastal and elevated areas.

2.2.2. Social data for vulnerability analysis

The people of Dacope Upazila in Khulna were the subjects of a semistructured questionnaire survey. The data were gathered using both quantitative and qualitative techniques. A random sampling technique was utilized to collect the survey data from nine unions of the Upazila to ensure spatial representation of the study area. Apart from the questionnaire, interviews with residents and official census records are the two main sources of information. A pilot (pretesting) survey was carried out before the questionnaire was finalized. For validity and reliability, survey questionnaires were reviewed by experts. Experts review the questionnaire to identify potential issues that the developer might have overlooked due to its proximity to the subject, such as ambiguous wording, bias, measurement errors, or administration problems (Ikart 2019). Experts were selected based on several criteria, first, their research area, such as social sociology and climate change. Second, the experts, who were assistant professors from the Department of Urban and Regional Planning, Khulna University of Engineering and Technology, had a relevant background. Finally, they have more than 3 years of experience in the research field, such as climate change.

Despite these measures, some potential biases may remain, including sampling bias and respondent bias. To minimize these biases, households from different geographic locations and socioeconomic backgrounds were included, and respondents were informed about the academic purpose of the study to reduce response bias.

2.3. Sample size calculation

Yamane (1967) suggests a simplified formula to estimate the sample size, which is applied under conditions where the size of the population is limited. If a 95% confidence level and $P = 0.05$ are assumed, the determining formula is given by (Yamane 1967; Kayes *et al.* 2025b)

$$n = \frac{N}{[1 + N(e)^2]} \tag{1}$$

where n is the desired sample size, N is the total population size, and e is the margin of error. The precision, i.e., margin of error, is considered to be 5% in the present study for the selection of households from the target population. Where the total population is denoted by $N = 152{,}316$, and the sample size for the research is $n = 159{,}362/\ (1 + 152{,}316\ (0.05)^2) = 399$.

By using the statistics from the 2022 national census, which estimated the total population of the upazila, 399 residences were surveyed in the Dacope. Upon the field team's arrival at the block, community leaders were informed about the study's purpose and asked to grant permission to visit homes. The survey was implemented in May 2024.

2.4. Climatic trend analysis

2.4.1. Mann–Kendall test

The Mann–Kendall (MK) test used for trend analysis is a nonparametric method (Mann 1945). It was used for the detection of statistically significant trends in variables like rainfall, temperature, and stream flow. Because it is robust to missing and irregularly spaced data, it does not require data to be normally distributed, and can detect monotonic trends without being impacted by outliers or time series length (Kamal & Pachauri 2018). To ascertain the presence of a statistically significant trend in climatic variables such as temperature and precipitation with reference to climate change, the nonparametric MK test was employed. The MK test checks the null hypothesis of no trend versus the alternative hypothesis of the existence of an increasing or decreasing trend. The statistics (S) are defined as

$$S = \sum_{i=1}^{N-1} \sum_{j=i+1}^{N} \operatorname{sgn}(x_j - x_i) \tag{2}$$

In Equation (2), N is the number of data points. Assuming $(x_j - x_i) = \theta$, the value of $\operatorname{sgn}(\theta)$ is computed as follow:

$$\operatorname{sgn} = \begin{cases} 1 & \text{if} \quad \theta > 0 \\ 0 & \text{if} \quad \theta > 0 \\ -1 & \text{if} \quad \theta > 0 \end{cases} \tag{3}$$

This statistic represents the number of positive differences minus the number of negative differences for all the differences considered. For large samples ($N > 10$), the test is conducted using a normal distribution, with the mean and the variance as follows:

$$E[S] = 0 \tag{4}$$

$$\operatorname{var}(S) = \frac{N(N-1)(2N+5) - \sum_{k=1}^{n} t_k(t_k-1)(2t_k+5)}{18}, \tag{5}$$

where n is the number of tied (zero difference between compared values) groups and t_k is the number of data points in the kth tied group. The standard normal deviate (Z statistic) is then computed as

$$Z = \begin{cases} \dfrac{S-1}{\sqrt{\operatorname{var}(s)}} S > 0 \, 0 \text{if} S > 0 \dfrac{S+1}{\sqrt{\operatorname{var}(S)}} \text{if} S > 0 \end{cases} \tag{6}$$

If the computed value of $|Z| > z\alpha/2$, the null hypothesis (H_0) is rejected at an α level of significance in a two-sided test. In this analysis, the null hypothesis was tested at a 95% confidence level.

Sen's slope estimation (Sen 1968) is another nonparametric method for trend analysis of a hydro climatic data set. It is used to detect the magnitude of the trend,

$$T_i = \frac{X_i - X_k}{J - k} \quad \text{For } i = 1, 2, 3, \ldots, N \tag{7}$$

In Equation (7), X_j and X_k are the data values for j and k times of a period, where $j > k$. The slope is estimated for each observation. Median is computed from N observations of the slope to estimate the Sen's slope estimator:

for N is odd
N is even (8)

'When the N Slope observations are shown as Odd, the Sen's Estimator is computed as Qmed = (N + 1)/2, and for Even times of observations, the Slope estimate is Qmed = [(N/2) + ((N + 2)/2)]/2. The two-sided test is carried out at 100(1 – α) % confidence interval to obtain the true slope for the nonparametric test in the series' (Mondal *et al.* 2012). The positive or negative slope Q_i is obtained as an upward (increasing) or downward (decreasing) trend.

2.4.2. RAI

To investigate rainfall variability in time, the RAI was used. Because it employs normalized precipitation values derived from a geographical area's historical record, it efficiently captures both positive and negative rainfall anomalies and offers a straightforward, trustworthy classification of wet and dry conditions (Raziei 2021). This procedure was first proposed by van Rooy in 1965, and its adapted form was proposed by Freitas (2005) and thereafter already applied in several research outputs, mainly in agricultural sciences. In this present study, RAI is applied to analyze the climate change scenario in Dacope. Rainfall anomalies are basically positive or negative; the formulas used in computing RAI in such situations are shown as follows (Costa & Rodrigues 2017):

$$\text{For positive, RAI} = 3\left|\frac{N - \bar{N}}{\bar{M} - \bar{N}}\right| \tag{9}$$

$$\text{For negative, RAI} = 3\left|\frac{N - \bar{N}}{\bar{X} - \bar{N}}\right| \tag{10}$$

In Equations (9) and (10), N represents the current yearly precipitation data (mm), $\bar{N}$ represents the early average precipitation (mm), $\bar{M}$ represents the average of the ten highest yearly precipitation (mm), and $\bar{X}$ represents the average of the ten lowest yearly precipitation(mm) from 1981 to 2021.

To facilitate a better understanding of the results, atmospheric conditions are categorized based on the Costa & Rodrigues (2017) study, which was adapted from the Freitas (2005) study. The classification by ranking the RAI value is shown in Table 1.

2.5. Construction of the SV index

Previous research by Ahsan & Warner (2014), Cutter *et al.* (2003), Das *et al.* (2020), Dintwa *et al.* (2019), Eakin & Bojorquez-Tapia (2008), Holand *et al.* (2011), Nguyen *et al.* (2017), and Otto *et al.* (2017a) indicated that SV is driven by very strong factors, which include age, sex, education, family income, occupation, savings, sanitation facilities, and household population density. The study utilized socioeconomic data about individuals and the status of the built environment in building methodologies. Social vulnerability index (SoVI) consisted of a collection of variables; for the study, a total of 28

Table 1 | Classification of RAI

Range of RAI	Classification into a group
>4	Extremely humid
2–4	Very humid
0–2	Humid
(−2)–0	Dry
(−4)–(−2)	Very dry
<(−4)	Extremely dry

Source: Freitas (2005) and Costa & Rodrigues (2017).

variables were selected, which are shown in Table 2. The indicators encompass the socioeconomic status of households, their financial situation, livelihood strategies, participation and affiliation with community-based organizations, and health status in connection to asset availability.

All SV variables were converted to *Z*-scores before doing the statistical analysis. PCA was used in making a composite index. PCA is a statistical technique to reduce a large set of variables into a small set of elements. Prior to conducting PCA, normalization is necessary because PCA is sensitive to the dataset's variable scale (Importance of feature scaling n.d.). Without normalization, variables with larger scales will dominate the principal components, and different variables may have wildly disparate units or ranges (Importance of feature scaling n.d.). Some variables, like age and the number of family members, cannot be scaled between 0 and 1. However, certain factors, such as having a cell phone, having a loan, and having cyclone shelters, are more conveniently represented by binary code, like 0 and 1. To gather the data, various coding techniques were used for every variable.

This analysis allows for the explanation of component groupings and looks at the components over time to determine if there are any changes in overall vulnerability. Because all variables were relatively well-spread across the Dacope Upazila, the PCA was very effective for this study. In doing the analysis, PCA created individual components that separately represented all the original components. Using PCA, these extracted components were computed to provide an SoVI for that upazila. This approach sets objective weights according to the variation explained by each component and aids in the removal of multicollinearity among variables. Therefore, compared with equal weighting or subjective weighting techniques, PCA offers a more dependable and data-driven strategy for assessing societal vulnerability; for this reason, this method was selected.

In the current study, PCA was carried out using the Statistical Package for Social Science, SPSS, v.25. The Kaiser criterion was followed, extracting only those principal components with eigenvalues superior to 1. The varimax rotation method was performed to enhance the interpretability of the components and to ensure more independent factors. Moreover, it is beneficial to reduce the number of heavily loaded variables into one component, which in turn increases the percentage variance among each of the factors. This was done iteratively until stable and statistically reliable components were obtained. Kaiser–Meyer–Olkin (KMO) measure of sample adequacy and Bartlett's test of sphericity were used in order to check the reliability of the model. A review of the results of the PCA was used to extract variables with the highest loadings within components from the rotated component matrix so as to understand the meaning of the independent components that were formed. Each element was designated with a name and a cardinality. Any factors that contribute to increased susceptibility were associated with positive indicators, and conversely, those that mitigate vulnerability were associated with negative indicators. Absolute values were assigned to those components that indicated a positive likelihood as well as a negative signal of SV. A composite score in the form of SoVI was computed by adding the score of each component. A summative approach was used to aggregate the individual scores of all the components. As there is no theoretical justification for weighting the components, the additive approach seemed to be the most pragmatic technique (Tasnuva *et al.* 2021). Therefore, the overall SoVI of the Dacope Upazila was calculated by adding the value of the major component:

$$\text{SoVI} = \sum \text{PC} \tag{10}$$

where SoVI denotes the SoVI and PC indicates the principal components that the varimax rotation extracted.

2.6. Future maximum temperature prediction

An intricate computer simulation tool used to forecast future climate conditions, including temperature, is called a global circulation model (GCM), sometimes referred to as a global climate model. The procedure of preparing the map is a four-step process.

Step 01: First up, downloading current and future climate data from the DIVA-GIS Global Climate Website.

Step 02: Then opening the shape file of the research area and addition of world climate data to DIVA-GIS.

Step 03: Then, from the data tab, the map through climate is opened to import climate data into the map. Both the current climate data and the future climate data of any climatic elements can be imported.

Step 04: Finally, the results are the map, representing current climatic elements (temperature, precipitation, and humidity) and 100-year future projection maps showing the change of different climatic elements.

Table 2 | Description of indicators selected for SoVI calculation

No	Indicator	Type	Name of indicator	Explanation	Relation/ sign	References
1	Household size	Continuous	HSIZ	Total household members	+	Notenbaert *et al.* (2013)
2	Age of the household head	Continuous	AGE	Age of household head (years)	+	Vincent & Cull (2010)
3	Dependency	Continuous	DEP	Number of household members those under 16 and those over 65.	+	Eakin & Bojorquez-Tapia (2008)
4	Female household member	Continuous	FEM	Total number of females in the HH.	+	Added by Researcher
5	Female household head	Binary	FEMHH	Gender of HH head. (female/ male = 1/0)	+	Hahn *et al.* (2009)
6	Number of girl children	Continuous	GC	Number of girl children in the household (age under 12 years)	+	Hahn *et al.* (2009)
7	Female with no education	Continuous	FNoEDU	Number of females with no education	+	
8	Housing type	Continuous	HOUSETYPE	Types of house (katha/semipucca/ pucca = 1/2/3)	–	Hahn *et al.* (2009)
9	Illness due to a natural disaster	Binary	ILLND	Illness faced due to natural disaster (yes/no = 1/0)	+	Hahn *et al.* (2009)
10	Single-headed family	Binary	SINGHD	Household having a single head (yes/no = 1/0)	+	Hahn *et al.* (2009)
11	Household having television	Binary	HTV	Household having a television (yes/no = 1/0)	–	Hahn *et al.* (2009)
12	Highest level of education	Ordinal	HEDU	Highest degree in HH	–	Eakin & Bojorquez-Tapia (2008)
13	Income	Continuous	INC	Gross monthly income	–	Piya *et al.* (2012)
14	Agricultural dependency	Continuous	AGRDEP	Percentage of monthly agricultural income in gross income	+	Piya *et al.* (2012)
15	Food struggle	Binary	HFS	Household struggled for food (yes/no = 1/0)	+	Hahn *et al.* (2009)
16	Number of months struggling for food	Continuous	NoHFS	Number of months struggling for food	+	Hahn *et al.* (2009)
17	Saving	Binary	SAV	Saving in the last 5 years (yes/no = 1/0)	–	Hahn *et al.* (2009)
18	Loan	Binary	LOAN	Loan access in the last 5 years for economic activities (yes/no = 1/ 0)	+	Eakin & Bojorquez-Tapia (2008)
19	Member of a community-based organization	Binary	CBO	Membership in community-based organization (yes/no = 1/0)	–	Eakin & Bojorquez-Tapia (2008)
20	Member of a micro credit organization	Binary	MMC	Membership in micro credit organization (yes/no = 1/0)	–	Hahn *et al.* (2009)
21	Virtual social network platform	Binary	SNP	Involvement with virtual social network platform (yes/no = 1/0)	–	Vincent & Cull (2010)

(*Continued.*)

Table 2 | Continued

No	Indicator	Type	Name of indicator	Explanation	Relation/ sign	References
22	Training in health care	Binary	THC	Received training on primary health care (yes/no = 1/0)	–	Hahn *et al.* (2009)
23	Time to reach primary school	Continuous	TTRPS	Time to reach the nearest primary school in minutes	+	Piya *et al.* (2012)
24	Household having mobile phone	Binary	MOB	Household having a mobile phone (yes/no = 1/0)	+	Vincent & Cull (2010)
25	Sewage	Binary	SEWAGE	Existence of a water sewage system (yes/no = 1/0)	–	Hahn *et al.* (2009)
26	Cyclone shelter	Binary	CYCLONESHELTER	Existence of a cyclone shelter within 2 km of the house	–	Modified
27	Ownership of land	Binary	LANDOWN	Have your own parcel of land (yes/no = 1/0)	–	Vincent & Cull (2010)
28	Time to reach the nearest vehicle station	Continuous	TTRVS	Time to reach the nearest vehicle station in minutes	+	Hahn *et al.* (2009)

2.6.1. Future climate projections (2 × CO_2 climate conditions, CCM3 model)

The future climate projections for Dacope Upazila were derived from the CCM3 (Canadian Climate Model version 3) model under the 2 × CO_2 climate conditions. The CCM3 was developed by the Canadian Centre for Climate Modelling and Analysis (CCCma), which is part of Environment and Climate Change Canada. The development of CCM3 was a collaborative effort involving several researchers, with one of the key papers being written by McFarlane *et al.* (1992), who are often credited with the development of the model. This model simulates climate conditions under a scenario where atmospheric carbon dioxide (CO_2) concentrations double compared with preindustrial levels, representing a significant increase in greenhouse gases. The future projections, derived from Govindasamy *et al.* (2003), are based on high-resolution global climate simulations, as described in their paper, 'High-resolution simulations of global climate, part 2: effects of increased greenhouse gases' published in Climate Dynamics (21: 391–404). These data were subsequently downscaled and matched to the WorldClim estimates of current climate by DIVA-GIS (Hijmans *et al.* 2005).

The 2 × CO_2 scenario typically leads to noticeable warming, which affects both temperature and precipitation patterns. Projections under this condition would likely show increased global temperatures, particularly over land areas, and changes in rainfall patterns (e.g., more intense rainfall events or shifts in seasonality). It is important to note that 2 × CO_2 may not necessarily represent the immediate future but could correspond to a medium-to-long-term future (e.g., 50–100 years from present), depending on current emission trajectories and policies (IPCC 2014).

The CCM3 is one of the global climate models (GCMs) used to simulate climate projections under different scenarios. GCMs like CCM3 are designed to represent the interactions between various components of the Earth's climate system, including the atmosphere, oceans, land surface, and ice. CCM3 typically has a coarse spatial resolution (e.g., around 2.8° × 2.8° grid), which means it captures global and regional climate trends but may not provide high-detail local projections (Flato *et al.* 2013).

The resolution of the downscaled projections used in this model is 2 minutes (~3.7 km). This high resolution helps capture more localized climate features, such as regional variations in temperature and precipitation, especially in areas with complex topography or coastal influences like Dacope. Using this resolution provides a finer level of detail than standard global models with coarser grids (e.g., 2.8° × 2.8°) and makes the projections more applicable for local climate analysis (Giorgi & Mearns 1999).

Methodological flowchart: The methodological flow chart is presented in Figure 2.

2.7. Data suitability for analysis

Precipitation data: Annual precipitation data distribution was tested using skewness, standard deviation, and kurtosis for 1981–2021. Kurtosis finds outliers, while skewness measures data distribution asymmetry. In 2017, rainfall peaked at

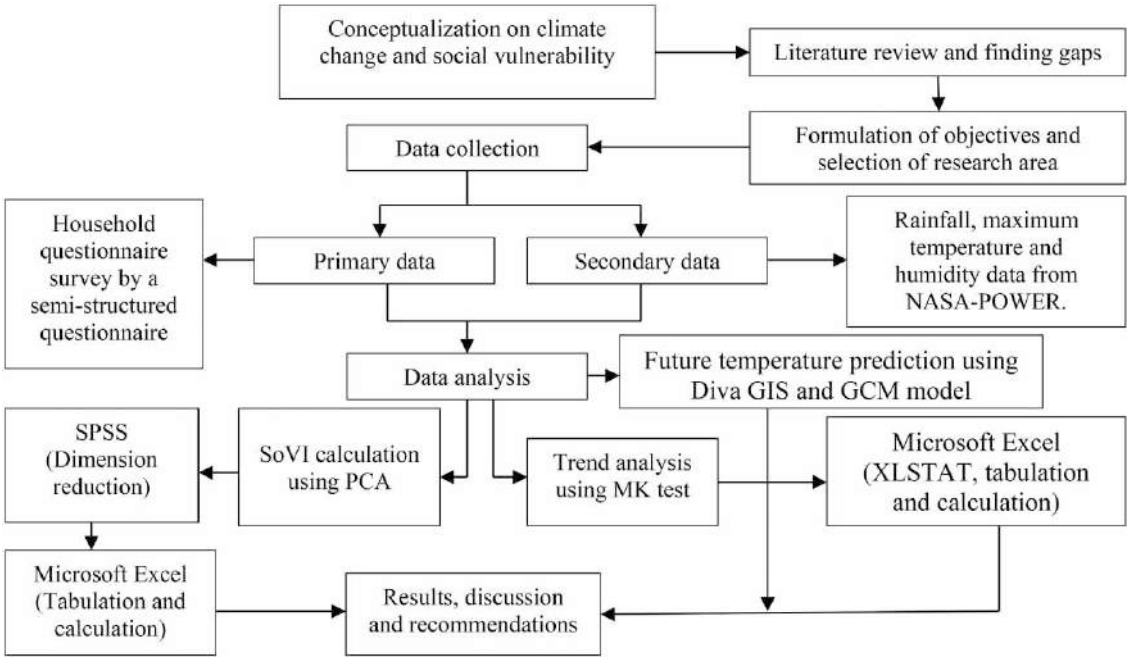

Figure 2 | Methodological Framework of the research.

3,796.88 mm. The lowest rainfall was 801.56 mm in 1983. Table 3 shows a moderate positive data skewness of 1.607. This means more years with lower precipitation and a few with exceptionally high values. For 27 of 41 years, annual rainfall was below average. In 36 years, from 1981 to 2021, the research region experienced less rainfall than Bangladesh's 2,427.7 mm. The data are right-skewed. Kurtosis of 2.723 reflects a 'platykurtic' distribution. Data distribution is platykurtic if kurtosis is less than 3. The distribution has a few fewer extreme values but is near normal.

Temperature data: The data distribution is considerably skewed to the left (negatively skewed), as indicated by the skewness score of −0.759 (Table 4). Consequently, the left tail of the distribution, or lower end, is longer or fatter than the right tail. The values on the higher side of the mean are less extreme, even though they are more numerous than those on the lower side. The distribution is considered 'platykurtic' as the kurtosis value is 0.346 and the excess form is

Table 3 | Statistical parameters of annual and seasonal precipitation patterns

Statistics		
Annual precipitation from 1981 to 2021		
N	Valid	41
	Missing	0
Mean		1,592.0566
Std. deviation		655.33035
Skewness		1.607
Std. error of skewness		0.369
Kurtosis		2.723
Std. error of kurtosis		0.724
Minimum		801.56 mm
Maximum		3,796.88 mm

Source: Authors' calculation, 2024.

Table 4 | Statistical parameters of annual maximum temperature pattern

Statistics		
Annual maximum temperature		
N	Valid	41
	Missing	0
Std. deviation		1.31925
Skewness		−0.759
Std. error of skewness		0.369
Kurtosis		0.346
Std. error of kurtosis		0.724
Minimum		38.69
Maximum		44.23

Source: Authors' calculation, 2024.

(0.346–3 = –2.654), which is <0. This further suggests that although the distribution is almost normal, it is less severe than a normal distribution by a small amount.

3. RESULTS AND FINDINGS

3.1. Trend analysis of mean precipitation

The MK test examined 1981–2021 rainfall trends in the study area. The results are in Table 5 and Figure 3. The MK test *Z* and *Q* values for monthly and annual rainfall are shown in Figure 3. Here in the table, ++++++ indicates very high significance at the 0.1% level; ++++ indicates significance at the 5% level and + indicates a statistically non-significant trend.

The analysis reveals both positive and negative trends in the time series data. Overall, annual rainfall has shown an upward trend, indicating an increase over the period. However, unseasonal rainfall has also increased. Notably, November to February is the winter season, yet the trends show positive or upward shifts for November and December, and negative or downward shifts for January and February (*Z* value: −0.096 and −0.042), although these shifts are not very significant.

Table 5 | Monthly precipitation trend analysis using the MK test and Sen's slope estimator

	Test				
Series	**Kendall's tau (*Z* value)**	**Shift**	**Sen's slope (*Q* value)**	***p*-Value**	**Significance level**
January	−0.096	Downward	0.000	0.430	+
February	−0.042	Downward	0.000	0.728	+
March	0.063	Upward	0.000	0.586	+
April	0.090	Upward	0.331	0.423	+
May	0.284	Upward	3.144	0.010	++ + +
June	0.263	Upward	4.038	0.017	++ + +
July	0.422	Upward	6.328	0.000	++ + ++ +
August	0.397	Upward	5.716	0.000	++ + ++ +
September	0.407	Upward	5.003	0.000	++ + ++ +
October	0.401	Upward	5.273	0.000	++ + ++ +
November	0.086	Upward	0.000	0.464	+
December	0.131	Upward	0.000	0.283	+
Annual	0.530	Upward	33.285	<0.0001	++ + ++ +

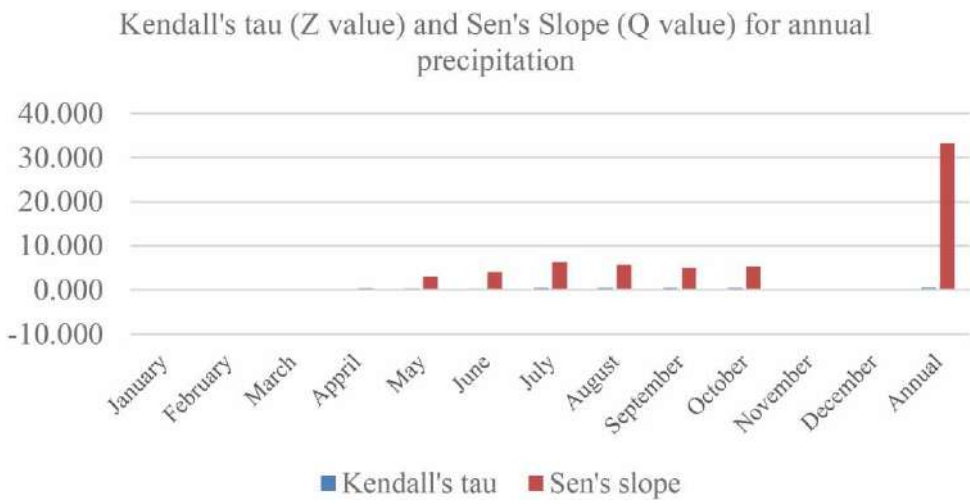

Figure 3 | Kendall's tau (*Z* value) and Sen's slope (*Q* value) for annual precipitation. *Source*: Authors' calculation, 2024.

Consequently, the risk of crop damage due to unseasonal rainfall has also increased, particularly affecting the harvesting period of Amon rice, which spans from November to December (Nelson *et al.* 2014). Additionally, the months of March (0.063), April (0.090), May (0.284), June (0.263), July (0.422), August (0.397), September (0.407), and October (0.401) are also showing an upward trend, signifying increased rainfall throughout the year.

3.2. RAI

To track the variation of rainfall from 1981 to 2021, the RAI was utilized, with the results presented in Table 6. The data indicate that over these 41 years, the study area experienced dry conditions for approximately 19 years and very dry conditions for 8 years. However, the last 6 years have seen a dramatic shift toward a more humid environment, with 3 years classified as extremely humid and the remaining 3 years as very humid. Consequently, the area has been increasingly affected by floods. This is corroborated by the annual flood reports of Bangladesh. In 2020, the country encountered floods that began in the latter part of June and lasted until July (Bangladesh Water Development Board 2020). In 2017, from April to August, flooding was triggered by unexpected early heavy rain in numerous regions of Bangladesh, particularly the Khulna district (Bangladesh Water Development Board 2020). The year with the highest negative value, indicating a very dry condition, was 1983, with a value of −3.9551. Conversely, the year with the highest positive value, indicating an extremely humid condition, was 2017, with a value of 7.1108.

3.3. Mean annual temperature

Mean annual temperature trend from the MK test shows a downward trend (*Z* value = −0.422) presented in Table 7. This means that the mean annual temperature has decreased over this period. The decrease in mean annual temperature has impacts on the community people's livelihood, adaptation strategies, and the ecosystem. The downward trend of mean annual temperature is shown in Figure 4. Here in the table, ++++++ indicates very high significance at the 0.1% level.

3.4. Monthly maximum temperature trend analysis

The study area's minimum temperature trends were examined using the MK test. Figures 5 and 6, as well as Table 8, exhibit the findings. Based on the MK test, Figure 5 presents a graphical depiction of Kendall's tau (*Z*) and Sen's slope (*Q*) values for monthly and annual minimum temperatures from 1981 to 2021. Here in the table, ++++++ indicates very high significance at the 0.1% level; ++++ indicates significance at the 5% level; +++ indicates marginal significance at the 10% level; ++ indicates weak or near-significant trend; and + indicates a statistically non-significant trend.

Annual and monthly maximum temperatures fall except in August (*Z* value is 0.021). Land surface evaporation may decrease with lower maximum temperatures (Bhuyan *et al.* 2018). The decline in evaporation may reduce atmospheric moisture, limiting monsoon rainfall (Bhuyan *et al.* 2018). Summer maximum temperatures are declining (Figure 5), but precipitation is rising (Figure 3). The research area's proximity to the Bay of Bengal and the number of rivers explain the

Table 6 | RAI for annual precipitation from 1981 to 2021

Year	Annual precipitation (*N*)	RAI	Classification
1981	1,861.52	0.86905	Humid
1982	1,392.19	− 1	Dry
1983	801.56	− 3.9551	Very dry
1984	1,233.98	− 1.7916	Dry
1985	954.49	− 3.19	Very dry
1986	1,439.65	− 0.7625	Dry
1987	1,249.8	− 1.7124	Dry
1988	1,197.07	− 1.9763	Dry
1989	817.38	− 3.876	Very dry
1990	1,339.45	− 1.2639	Dry
1991	933.4	− 3.2955	Very dry
1992	938.67	− 3.2691	Very dry
1993	1,197.07	− 1.9763	Dry
1994	970.31	− 3.1108	Very dry
1995	1,228.71	− 1.818	Dry
1996	970.31	− 3.1108	Very dry
1997	1,355.27	− 1.1847	Dry
1998	1,576.76	− 0.0765	Dry
1999	1,576.76	− 0.0765	Dry
2000	1,481.84	− 0.5515	Dry
2001	1,592.58	0.00169	Humid
2002	1,371.09	− 1.1056	Dry
2003	1,307.81	− 1.4222	Dry
2004	1,450.2	− 0.7098	Dry
2005	1,144.34	− 2.2401	Very dry
2006	1,281.45	− 1.5541	Dry
2007	2,035.55	1.43032	Humid
2008	1,502.93	− 0.4459	Dry
2009	1,787.7	0.63097	Humid
2010	1,592.58	0.00169	Humid
2011	1,766.6	0.56292	Humid
2012	1,249.8	− 1.7124	Dry
2013	1,898.44	0.98812	Humid
2014	1,350	− 1.2111	Dry
2015	2,025	1.39629	Humid
2016	3,032.23	4.64472	Extremely humid
2017	3,796.88	7.1108	Extremely humid
2018	2,278.12	2.21263	Very humid
2019	3,142.97	5.00187	Extremely humid
2020	2,700	3.57324	Very humid
2021	2,451.86	2.77296	Very humid

Table 7 | Mean annual temperature trend analysis using the MK test and Sen's slope estimator

	Test				
Series	**Kendall's tau (*Z* value)**	**Shift**	***p*-Value**	**Sen's slope**	**Significance level**
Mean annual temperature	−0.422	Downward	0.000	−0.024	++ + ++ +

Source: Authors' calculation, 2024.

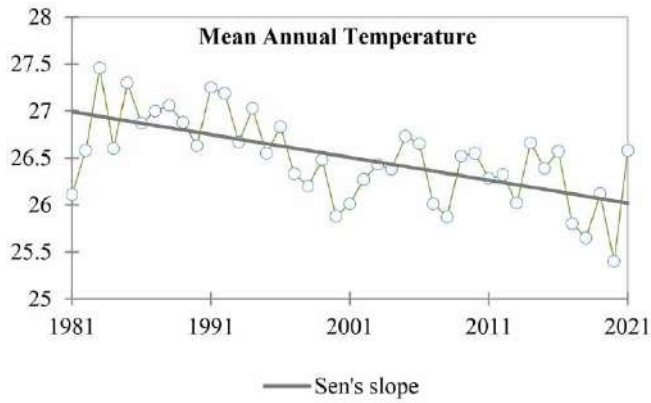

Figure 4 | Annual temperature trend for the period 1981–2021 on an annual basis in Dacope.

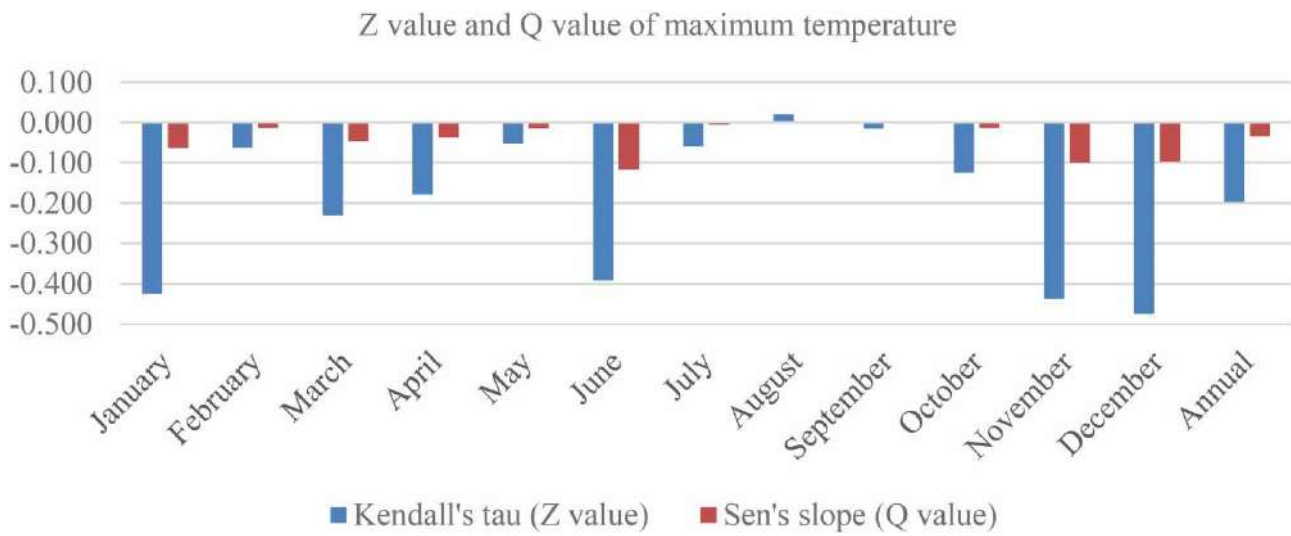

Figure 5 | MK statistics (*Z* value) and Sen's slope (*Q* value) for different months and seasons of minimum temperature. *Source*: Authors' calculation, 2024.

disparity. Heat is absorbed by water during the day and released slowly at night (Chaidez *et al.* 2017). This does not prove it, but these water bodies' thermal qualities may raise minimum temperatures. Figure 6 shows monthly and annual maximum temperatures.

3.5. Future projection of average maximum temperature

The further elucidation of the average maximum temperature depicts with future projections and explains that there is a remarkable warming trend that negatively impacts the climate vulnerability and adaptive capacity. The spatial analysis, which is carried out based on Diva GIS and general circulation model (GCM) outputs for the year 2100, indicates that in the entire upazila, there is an evident increase in maximum temperatures.

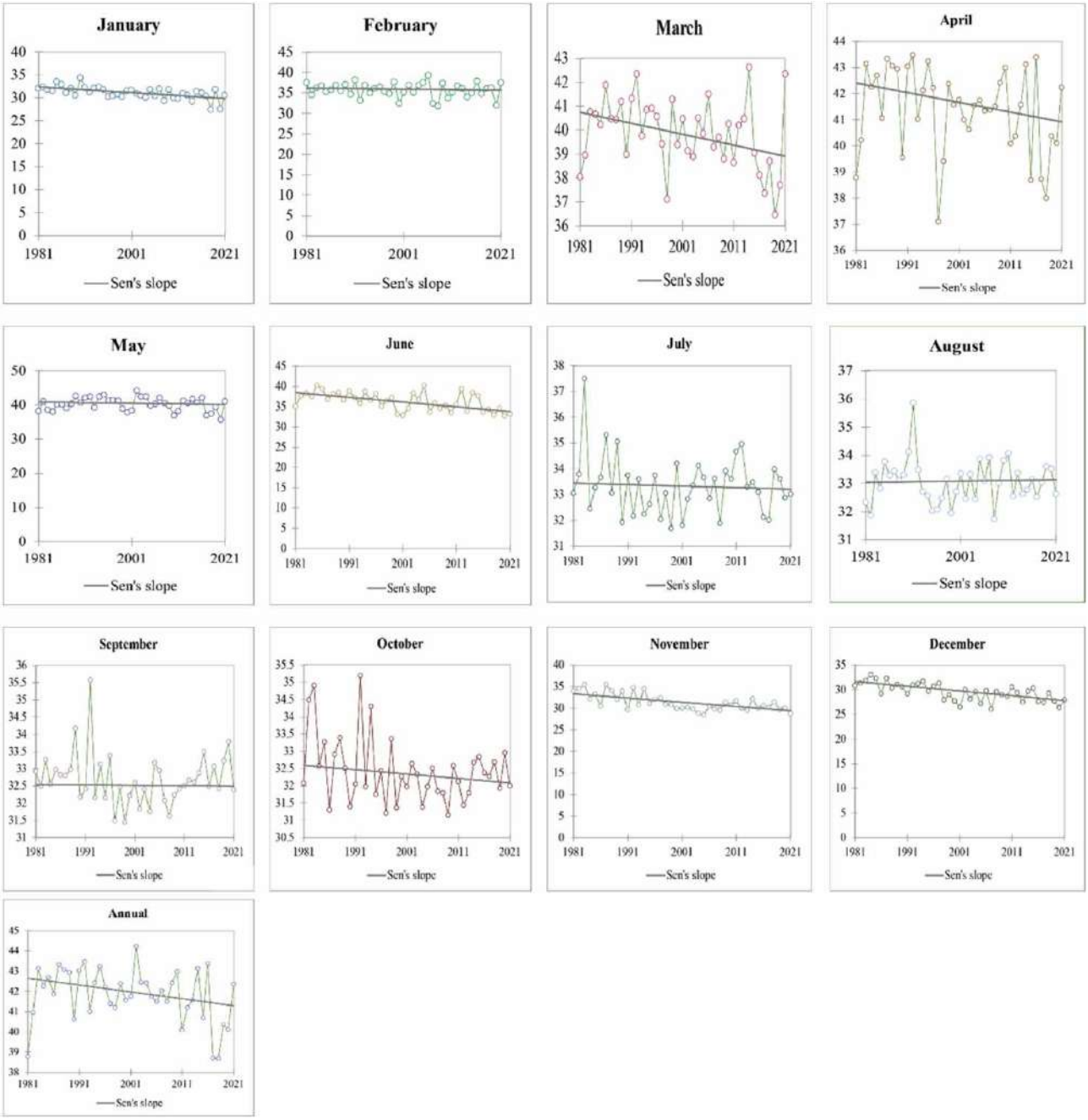

Figure 6 | Linear maximum temperature trends for the period 1981–2021 on a monthly and annual basis. *Source*: Authors' illustration, 2024.

The current average maximum temperature map (Figure 7) reveals a thermal gradient along latitudinal lines, i.e., it is lower along the southern coast belt (30.0–30.40 °C depicted in green) and higher (up to 31.00 °C represented in red) in the northern inland regions. This pattern holds with the concept of the moderating effect of the Bay of Bengal to the south and a greater extent of warming in central and Northwest.

On the contrary, the future average maximum temperature map (2100) indicates an overall increase in the range of temperature in all regions of Dacope (Figure 8). Areas in the south, in the lower range (30.0–30.5 °C), are projected to be above 31.5 °C, and areas in the North, which already have a warmer climate, are likely to be 33.0 °C and above. The extensive thermal amplification or intensification implies a lack of cooling protection hitherto provided by the coastline, meaning the homogenization of the heat stress throughout the upazila.

Table 8 | Maximum temperature trend analysis using the MK test and Sen's slope estimator

	Test				
Series	**Kendall's tau (*Z* value)**	**Shift**	***p*-Value**	**Sen's slope (*Q* value)**	**Significance level**
January	– 0.425	Downward	< 0.0001	– 0.063	+ + + + + +
February	– 0.062	Downward	0.574	– 0.013	+
March	– 0.231	Downward	0.035	– 0.047	+ + + +
April	– 0.178	Downward	0.103	– 0.038	+ +
May	– 0.052	Downward	0.637	– 0.014	+
June	– 0.392	Downward	0.000	– 0.117	+ + + + + +
July	– 0.059	Downward	0.597	– 0.006	+
August	0.021	Upward	0.857	0.003	+
September	– 0.015	Downward	0.902	– 0.001	+
October	– 0.125	Downward	0.256	– 0.013	+
November	– 0.439	Downward	< 0.0001	– 0.100	+ + + + + +
December	– 0.475	Downward	< 0.0001	– 0.098	+ + + + + +
Annual	– 0.198	Downward	0.070	– 0.034	+ + +

Source: Authors' calculation, 2024.

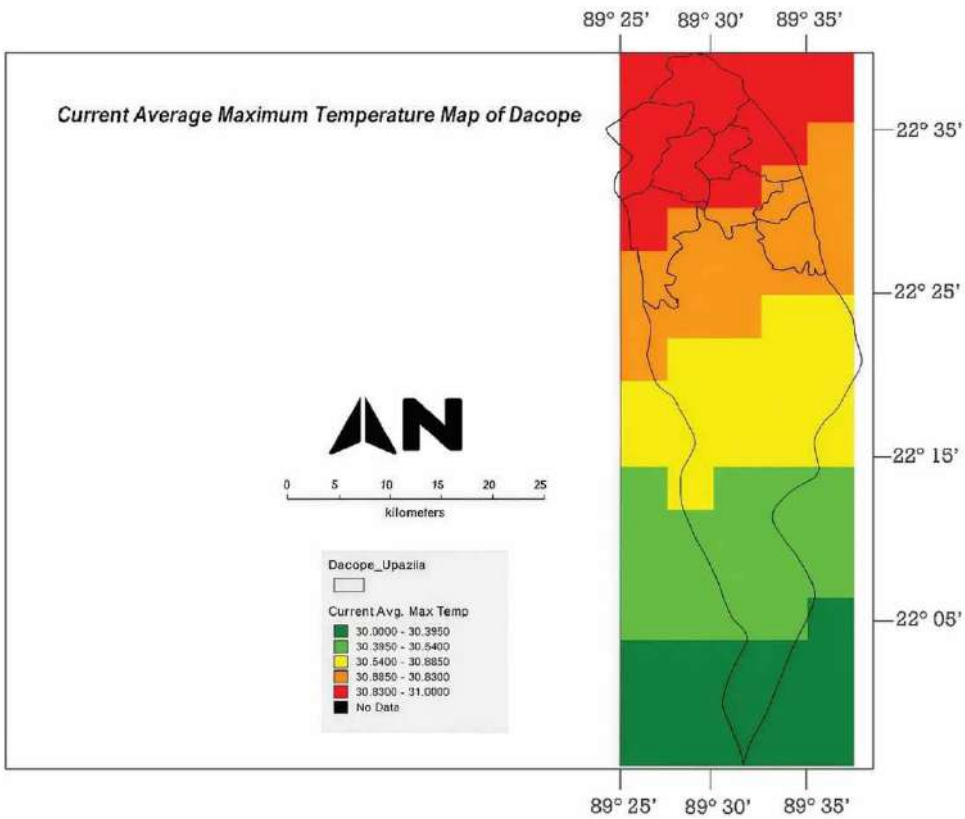

Figure 7 | Current average maximum temperature map.

This situation intensifies as reported in the difference map (Figure 9), indicating expected increases in temperature of between +1.0 and +2.0 °C in maximum temperatures. It is worthwhile to mention that the northernmost unions reveal the most significant growth (1.6–2.0 °C, shown in red), which means they are highly exposed to the extreme impact of

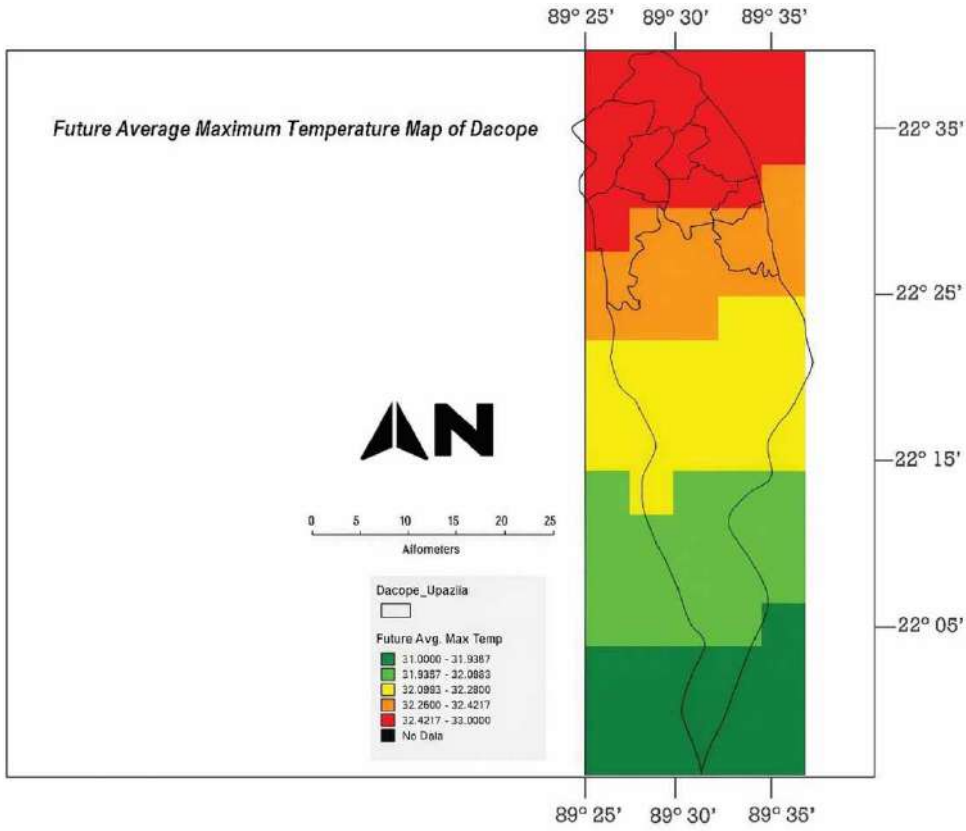

Figure 8 | Future average maximum temperature map.

warmer climate conditions. Areas along the coast in the south are a little less warming (1.0–1.50 °C), but the temperature level can still be observed as going up.

This anticipated rise in average maximum temperature will have a probable impact of enhancing previous cases of vulnerability in Dacope, especially in the sectors that rely on climate-sensitive activities like the agricultural sector, aquaculture, and water resource management. The maximum temperatures could have a stressful effect on rice and shrimp production lifecycle, a decrease in the yields of crops, promote heat stress in livestock, and worsen the quality of freshwater. Human health, in addition, there may be increased risk to human health due to extreme weather conditions, or increased risk to health due to the spread of mosquitoes that cause the infection. Cooling electricity demand and degradation of infrastructures, especially those in the education and health sectors, might arm it with burdens as well. These results have highlighted the necessity of tailored adaptation options, such as heat-resistant crop strains, better water resource management, and an early warning system in the community. Such anticipated alterations in Dacope should be taken into account within the context of planning the climate-resilient development to minimize the risks over the long term and increase the local adaptive capacity.

3.6. SoVI calculation

Experts have developed multiple indices to assess vulnerability, such as the composite vulnerability index (Wells 1997), commonwealth vulnerability index (Atkins *et al.* 2000), SoVI (Cutter *et al.* 2003), socioeconomic vulnerability index, the built environment vulnerability index (Holand *et al.* 2011), and others. One frequently used and dependable measure for assessing vulnerability is the SoVI, which was created by Cutter *et al.* (2003). Despite a few limitations, the SoVI framework has become widely accepted and popular because of its utilization of publicly accessible census data and construction methodologies, as well as its straightforward interpretation of intricate SV concepts (Spielman *et al.* 2020).

The study utilized a set of 28 variables to construct the SoVI. PCA was utilized to construct a composite index. PCA is a statistical method employed to condense a vast array of variables into a more concise set of elements (Kaźmierczak

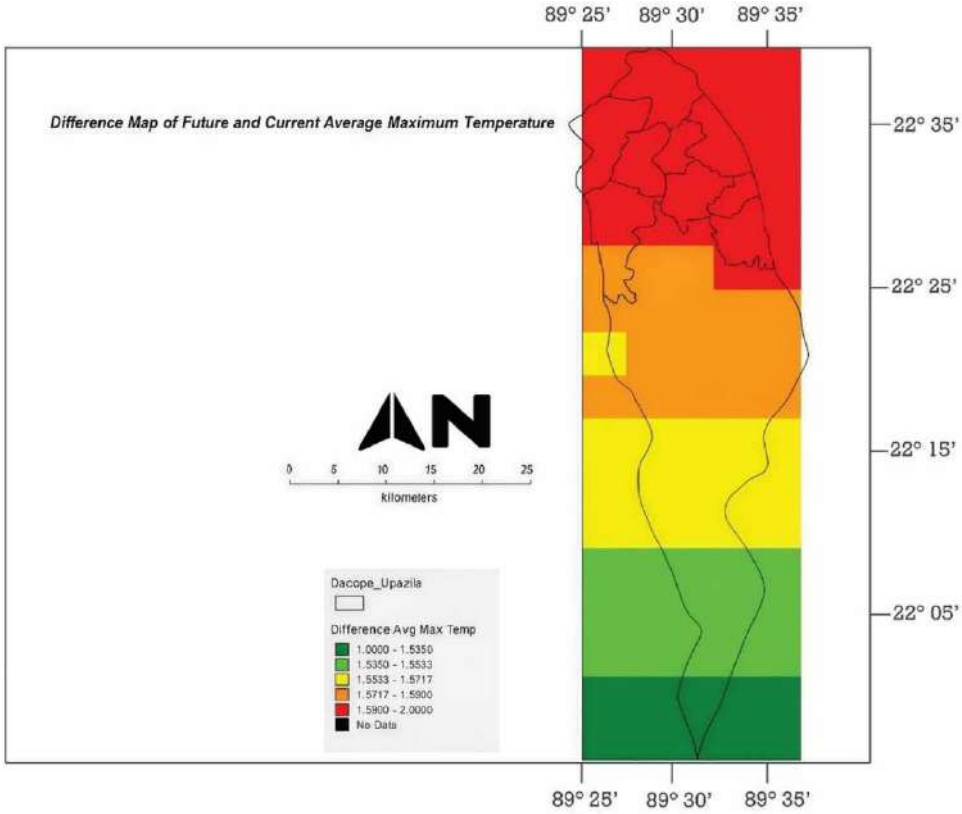

Figure 9 | Comparison of current and future average maximum temperature.

& Cavan 2011; Bodrud-Doza *et al.* 2016). This analysis facilitates the elucidation of component groupings and investigates the components over a period of time to determine if there are any alterations in overall vulnerability. Given that all 28 variables were evenly distributed among the nine unions of the Dacope Upazila, the PCA was highly effective for this study. During the analysis, PCA generated individual components that collectively represented all the initial components. Subsequently, the extracted components obtained through PCA were utilized to compute an SoVI for the upazila.

PCA was conducted using the Statistical Package for Social Science (SPSS, v.25). The Kaiser criterion was used to extract principal components, and only the components with eigenvalues greater than 1 were retained. The Varimax rotation method was employed to facilitate the interpretation of the components and generate a greater number of independent factors. Additionally, it is beneficial to reduce the number of heavily loaded variables into a single component, which in turn increases the percentage variance among each of the factors (Armaș & Gavriș 2013; Islam & Ahmed 2018). This method was implemented iteratively until stable and statistically reliable components were identified. The KMO measure of sample adequacy and Bartlett's test of sphericity were employed to assess the reliability of the model. The PCA findings were used to extract variables with the highest loadings within components from the rotated component matrix in order to identify the meaning of the independent components that were formed. Every element was given a name and a cardinality. The factors that contribute to increased susceptibility were associated with positive indicators, whereas those that decrease vulnerability were associated with negative indicators. Absolute values were assigned to the components that had both a positive and a negative indication of SV likelihood. A composite SoVI score was computed for the upazila by summing the scores of each component. The overall SoVI for the Dacope Upazila was determined by summing the value of the major components:

$$\text{SoVI} = \text{PC1} - \text{PC2} + \text{PC3} - \text{PC4} - \text{PC5} - \text{PC6} + \text{PC7} + \text{PC8}$$

3.7. SoVI for Dacope Upazila

PCA yielded ten components with eigenvalues over 1.0. The primary components account for 71.09% of the overall variability in the data. The variables with the highest component loadings were selected as the primary drivers of the factors. All the similarities had a value larger than 0.50. The KMO test value was 0.683, indicating moderate sampling adequacy. Additionally, Bartlett's test of sphericity was statistically significant at a significance level of $p < 0.05$. This suggests that the variables utilized in this investigation were suitable for PCA. In addition, the seven components were designated according to the variables that were loaded and their cardinality. These components are population vulnerability, service access, disaster and impact, assets and infrastructure, social network and economic resilience, liabilities, and natural resources. Table 9 displays concise explanations of the seven components.

The overall SoVI score for Dacope Upazila was calculated by summing all seven components. The SoVI score for Dacope Upazila is +8.772, indicating its overall performance. Since the SoVI value is positive, it indicates that Dacope Upazila has a significantly high level of social sensitivity to climate change.

3.8. Factors influencing SV in Dacope Upazila

Table 9 presents eight principal components with eigenvalues corresponding to the total amount of variance contributing to the SoVI. If we look at each factor in its component, we can establish what the primary catalysts of SV are.

The first principal component, named Household Vulnerability and Demographic Dynamics, comprises eight drivers with an eigenvalue of 8.294 and accounts for 19.239% of the contribution. The variables that comprise this component include the age of the household head, whether it is a single household head, the size of the household, the number of female members, the dependency ratio, the number of girl children, the struggle to find food, and the number of months spent struggling

Table 9 | Results of PCA for developing the SoVI of Dacope Upazila

Component no.	Component name	Eigen value	No. drivers	Variables	Loading	Relation with vulnerability	Cardinality and PC value	Explained variance
PC1	Household vulnerability and demographic dynamics	8.294	8	FEM	0.897	+	+ 6.056	19.239
				DEP	0.880	+		
				HSIZ	0.725	+		
				NoHFS	0.626	+		
				HFS	0.616	+		
				GC	0.698	+		
				AGE	0.878	+		
				SINGHD	0.736	+		
PC2	Household economic status and asset ownership	6.215	5	HOUSETYPE	0.494	–	– 0.003	14.416
				INC	0.462	–		
				SAV	– 0.706	–		
				LANDOWN	0.454	–		
				HTV	– 0.701	–		
PC3	Access and disaster health impact	4.853	3	TTRVS	0.808	+	+ 2.314	11.257
				ILLDS	0.798	+		
				TTRPS	0.708	+		
PC4	Education and digital connectivity	4.536	3	HEDU	0.654	–	– 0.528	10.521
				SNP	0.400	–		
				MOB	– 0.526	–		
PC5	Safety preparedness	2.389	3	CYCLONESHELTER	0.465	–	– 1.400	5.543
				THC	0.452	–		
				SEWAGE	0.483	–		
PC6	Source of finance	1.875	2	MMC	0.506	–	– 0.898	4.349
				CBO	0.392	–		
PC7	Agricultural finance	1.358	2	AGRDEP	0.883	+	+ 1.625	3.150
				LOAN	0.742	+		
PC8	Females participation	1.121	2	FNoEDU	0.818	+	+ 1.604	2.600
				FEMHH	0.786	+		

Source: Authors' calculation, 2024.

for food. Given that each of these indicators indicates heightened susceptibility, we designate this primary factor with a positive symbol (+).

The second principal component is household economic status and asset ownership, with five drivers and an eigenvalue of 6.215, adding 14.416% to SV. The drivers include an increase in the types of houses, income, savings, the presence of televisions in households, and the ownership of land. The majority of the houses in that area are made of katcha materials, such as tin sheets, gulpatha, or straw walls. The income of the people in that area is primarily dependent on nature, and the majority of households live below the extreme poverty line. Since all of these drivers have a negative impact on vulnerability, this component is also assigned a negative sign (–).

The third principal component is access and disaster health impact, with an eigenvalue of 4.853; it explains 11.257% of SV. It computed four variables: time to reach the nearest vehicle station, illness from a natural disaster, and time to reach the nearest primary school. Being a coastal area, this area frequently experiences natural disasters, which in turn bring with them a wave of illnesses. This area is crisscrossed with rivers, and the distance between the house and the primary school, market, and vehicle station is too long. We attach the plus sign (+) to this variable because it positively contributes to SV.

The fourth principal component, 'Education and Digital Connectivity,' has a contribution of 4.536 and an eigenvalue of 10.521% to the total variance. Factors influencing this component include the highest level of education, the virtual social networking platform, and households with mobile phones. Despite the prevalence of mobile phones in most households, smartphones remain uncommon. People are familiar with social media, but those pursuing higher education typically use it in remote areas. All these factors have a negative impact on this component; as a result, it is labeled as negative (–).

The fifth principal component is thematically named 'safety preparedness,' with an eigenvalue of 2.389 contributing 5.543% to the total variance. The use of cyclone shelters, sewage management, and primary healthcare training comprises this component. A cyclone shelter is essential during a natural disaster, but the distance is a matter of concern. More distance increases risk and vulnerability. As this area experiences frequent disasters, primary healthcare training reduces risk and vulnerability, and vice versa. Health facilities are scarce in this area. In accordance with this, the component is also assigned a negative sign.

The sixth principal component is 'source of finance,' which has two constituents: membership in a microcredit organization and membership in a community-based organization. This component's eigenvalue is 1.875, which contributes 4.349% to the total variance. These two sources are the main sources of finance to fight the vulnerability in this area and face lots of challenges in repaying the loan amount. However, these two sources help with the time of need and the loan amount they provide at the micro level, reducing vulnerability. This factor is classified as negative (–) due to its negative correlation with vulnerability.

The seventh principal component, 'agricultural finance,' consists of only two factors: the household's land ownership and its loan status. Its eigenvalue is equal to 1.358, and it contributes 3.150% to the total variance. The majority of the population lives below the extreme poverty line and lacks the capital to cultivate, lease, or contract land. In that scenario, they must obtain a loan. The findings also indicate that nearly all households bear the burden of debt, leading to a gradual increase in their vulnerability over time. Vulnerability directly correlates with this variable, which is why the component bears a positive (+) sign.

In terms of social aspects, women are the most vulnerable group in coastal areas. Women lag behind in areas such as education, community engagement, and employment. The final principal component, 'female's participation,' encompasses two variables: the uneducated female household member and the female head of the household. The eigenvalue for this principal component is 1.121, and it contributes 2.6% to the variance. At the primary level, and occasionally at the higher secondary level, women have the opportunity to pursue education. In some cases, these women have progressed to pursue higher education and jobs. However, a significant portion of women remain unaffected by education, thereby increasing their vulnerability. Vulnerability directly correlates with this variable, which is why the component bears a positive (+) sign.

4. DISCUSSION

When the air is very humid, people feel hotter because the body's natural way of cooling down, sweating, does not work as well (Outstandingdev 2025). According to Hasan *et al.* (2025c), 81% of the people of Dacope Upazila feel the temperature of the area has increased in recent years. In this study, RAI results highlighted that in the last 5 years, the environment turned from dry to extremely humid. This completely supports the findings of Hasan *et al.* (2025c) and the relation between

humidity and temperature. This also indicates that thermal discomfort in the study area may be driven more by increasing humidity than by increases in maximum temperature, which explains why local people perceive rising temperatures even though the maximum temperature trend shows a decrease. Alongside, high humidity does contribute to increased rainfall (Ido 2025). From the trend analysis of this research for monthly and annual precipitation, we found an upward trend, which supports the scientific statement of the relationship between rainfall and humidity. This increasing trend of rainfall is consistent with the hydro-climatic characteristics of coastal Bangladesh, where increased atmospheric moisture often results in higher precipitation.

The ocean and mangroves play a pivotal role in the hydrological cycle, which makes it rain more and lowers temperatures both locally and globally (Wilson n.d.; Byrne *et al.* 2016). The study area is located close to the Bay of Bengal and the Sundarban mangrove forest (the largest mangrove forest in the world). This also aligns with the findings of this study. The presence of the Bay of Bengal and the Sundarbans may contribute to higher evapotranspiration, increased cloud cover, and reduced solar radiation, which can lead to lower daytime maximum temperatures in coastal regions. The trend analysis of this study for the monthly and annual maximum temperature showed that the temperatures are decreasing. Hossain *et al.* (2013) and Jihan *et al.* (2025) forecasted an increase in Bangladesh's temperature by 1.0–5.0 °C. This study predicted that the temperature would rise by 1–2 °C, and the results of this study support the prediction of Hossain *et al.* (2013) and Jihan *et al.* (2025). However, the observed decreasing trend in maximum temperature suggests that local-scale climatic conditions in coastal areas may differ from national-scale projections due to maritime influence and mangrove-induced cooling effects. This highlights the importance of local environmental factors in climate trend analysis.

According to Bergstrand *et al.* (2014) and Mattah *et al.* (2023), SV is usually caused by a mix of economic, demographic, and social traits that make it harder for people and communities to prepare for, deal with, resist, and recover from different dangers or threats. Their findings completely align with the findings of this research. In this research, we found that demographic, economic, and social aspects are the most significant contributing factors for SV. This implies that climate-related factors such as increasing humidity and rainfall may further exacerbate SV, particularly for economically and socially disadvantaged groups, indicating a strong interaction between environmental change and socioeconomic sensitivity in the coastal region.

5. CONCLUSION

Bangladesh is quite susceptible to the effects of climate change, which could bring about a variety of natural disasters such as flooding (both riverine and flash), tropical cyclones, surges of water, droughts, salt intrusions, rising sea levels, and erosion of riverbanks and coastlines. This paper's trend analysis answered the first question of the research that the country's resources for water, public health, livestock, fisheries, agriculture, food security, and overall human wellbeing are all greatly affected by temperature and precipitation fluctuations. Climate change has widespread and comprehensive impacts, leading to an increase in the severity, frequency, and length of natural disasters. As a result, marginalized people are becoming highly susceptible to these events. This study aims to develop an SV index for households in the Dacope Upazila of southwest coastal Bangladesh using the SoVI methodology. This study presents the results of the SV analysis for each indicator, as well as the scores for the SoVI, specifically focusing on the southwest coastal region. The results of this study answered the second and third research questions that vulnerability is influenced by both natural determinants and social interactions. The SV, or social vulnerability, must be integrated into the comprehension of the interactions that expose individuals to potential dangers associated with hazards.

The results of this study are essential for decision-makers to design an effective and systematic policy for the examined union and the entire coastal region, which lacks comprehensive social resources to adjust to locations with a lack of distinct social capital, as demonstrated by our research. Therefore, a strategy to decrease vulnerability should prioritize vocational diversification and establish other sources of income for coastal residents who are now experiencing a precarious situation. Decision-makers should prioritize addressing population-based issues in places, while also focusing on addressing a composite SV in the coastal region.

5.1. Limitations of the study

This study has been limited by the lack of local-level data from the Bangladesh Meteorological Department (BMD) due to the absence of weather stations in Dacope Upazila. As a result, the study uses satellite data from NASA's POWER project. The results may be somewhat different from those found at the district level in Khulna because of this.

5.2. Future areas of research

Future research may concentrate on evaluating methods to enhance the income levels of local communities in Dacope, identifying suitable adaptation strategies to alleviate the effects of increasing temperatures, and investigating ways to bolster the region's climate resilience.

ACKNOWLEDGEMENTS

We would like to express our heartfelt gratitude to all the individuals who generously shared their valuable insights, experiences, and data that were integral to the success of this research.

AUTHORSHIP CONTRIBUTION STATEMENT

Md. Kamrul Hasan: conceptualization, investigation, data curation, methodology, software, and writing – original draft.
Md. Mizanur Rahman: resources, supervision, writing – review and editing, and validation.
Abu Nayem Md. Kayes: formal analysis, writing – original draft, data presentation, software, and methodology.

DECLARATION OF CONFLICTING INTERESTS

The authors declared no potential conflicts of interest with respect to the research, authorship, and/or publication of this article.

ETHICS STATEMENT

Ethics approval was obtained from the Ethics Committee of the Department of Urban and Regional Planning, Pabna University of Science and Technology (Bangladesh). In addition, the participants provided their informed consent to participate in this study.

CLINICAL TRIAL

Clinical trial number: Not Applicable.

FUNDING STATEMENT

The research was conducted under the funding of the University Grant Commission, Bangladesh.

DATA AVAILABILITY STATEMENT

Data cannot be made publicly available; readers should contact the corresponding author for details.

CONFLICT OF INTEREST

The authors declare there is no conflict.

REFERENCES

Ahmed, A. U., Neelormi, S. & Rahman, A. (2019) *Vulnerability and Adaptation to Climate Change in Bangladesh*. Washington, D.C., United States: World Bank.

Ahsan, M. N. & Warner, J. (2014) The socioeconomic vulnerability index: a pragmatic approach for assessing climate change led risks - a case study in the south-western coastal Bangladesh, *International Journal of Disaster Risk Reduction*, **8**, 32–49. https://doi.org/10.1016/j.ijdrr.2013.12.009.

Alam, M. & Collins, A. (2010) Cyclone disaster vulnerability and response experiences in coastal Bangladesh, *Disasters*, **34** (4), 931–954. doi:10.1111/j.1467-7717.2010.01176.x.

Armaș, I. & Gavriș, A. (2013) Social vulnerability assessment using spatial multi-criteria analysis (SEVI model) and the social vulnerability index (SoVI model)–a case study for Bucharest, Romania, *Natural Hazards and Earth System Sciences*, **13** (6), 1481–1499. doi:10.5194/nhess-13-1481-2013.

Atkins, J. P., Mazzi, S. A. & Easter, C. D. (2000) Commonwealth vulnerability index for developing countries: the position of small states, *Economic Paper*. Article no 29. https://doi.org/10.14217/23101385.

Bangladesh Water Development Board (2020) *Flood Situation Report 2020*. Dhaka, Bangladesh: Bangladesh Water Development Board. Available at: https://www.bwdb.gov.bd/archive/pdf/Flood%20Situation%20Report%202020.pdf.

BBS (2023a) POPULATION AND HOUSING CENSUS 2022. In BBS. Available at: https://bbs.portal.gov.bd/sites/default/files/files/bbs.portal.gov.bd/page/b343a8b4_956b_45ca_872f_4cf9b2f1a6e0/2024-01-31-15-51-b53c55dd692233ae401ba013060b9cbb.pdf.

Bergstrand, K., Mayer, B., Brumback, B. & Zhang, Y. (2014) Assessing the relationship between social vulnerability and community resilience to hazards, *Social Indicators Research*, **122** (2), 391–409. https://doi.org/10.1007/s11205-014-0698-3.

Bhuyan, M. D. I., Islam, M. M. & Bhuiyan, M. E. K. (2018) A trend analysis of temperature and rainfall to predict climate change for northwestern region of Bangladesh, *American Journal of Climate Change*, **07** (02), 115–134. https://doi.org/10.4236/ajcc.2018.72009.

Bodrud-Doza, M., Islam, A. R. M. T., Ahmed, F., Das, S., Saha, N. & Rahman, M. S. (2016) Characterization of groundwater quality using water evaluation indices, multivariate statistics and geostatistics in central Bangladesh, *Water Sciences*, **33** (1), 19–40. https://doi.org/10.1016/j.wsj.2016.05.001.

Byrne, D., Garcia-Soto, C., Hamilton, G., Leuliette, E., Lisan, Y., Campos, E., Durack, P. J., Manzella, G. M. R., Tadokoro, K., Schmitt, R. W., Arkin, P., Bryden, H., Nurse, L. & Milliman, J. (2016) Chapter 4. The Ocean's role in the Hydrological Cycle (By L. Inniss & P. Bernal). Available at: https://www.un.org/depts/los/global_reporting/WOA_RPROC/Chapter_04.pdf.

Chaidez, V., Dreano, D., Agusti, S., Duarte, C. M. & Hoteit, I. (2017) Decadal trends in Red Sea maximum surface temperature, *Scientific Reports*, **7** (1), 7146. https://doi.org/10.1038/s41598-017-08146-z.

Chowdhury, K. J., Ali, M. R., Chowdhury, M. A. & Islam, S. L. U. (2024b) Climate change induced risks assessment of a coastal area: a 'socioeconomic and livelihood vulnerability index' based study in coastal Bangladesh, *Natural Hazards Research*, **5**, 75–87. https://doi.org/10.1016/j.nhres.2024.06.005.

Cooper, N. (2023) *Climate Change: The IPCC Just Published Its Summary of 5 Years of Reports – Here's What You Need to Know*. Cologny, Switzerland: World Economic Forum. Available at: https://www.weforum.org/stories/2023/03/the-ipcc-just-published-its-summary-of-5-years-of-reports-here-s-what-you-need-to-know/.

Costa, J. A. & Rodrigues, G. P. (2017) Space-time distribution of rainfall anomaly index (rai) for the Salgado Basin, ceará state – Brazil, *Ciência E Natura*, **39** (3), 627. https://doi.org/10.5902/2179460 (26080.

Cutter, S. L., Boruff, B. J. & Shirley, W. L. (2003) Social vulnerability to environmental hazards*, *Social Science Quarterly*, **84** (2), 242–261. https://doi.org/10.1111/1540-6237.8402002.

Das, S., Hazra, S., Haque, A., Rahman, M., Nicholls, R. J., Ghosh, A., Ghosh, T., Salehin, M. & Safra De Campos, R. (2020) Social vulnerability to environmental hazards in the Ganges-Brahmaputra-Meghna delta, India and Bangladesh, *International Journal of Disaster Risk Reduction*, **53**, 101983. https://doi.org/10.1016/j.ijdrr.2020.101983.

Didar-Ul Islam, S. M., Bhuiyan, M. A. H. & Ramanathan, A. L. (2015) Climate change impacts and vulnerability assessment in coastal region of Bangladesh: a case study on Shyamnagar Upazila of Satkhira District. Content.Iospress.Com. https://doi.org/10.3233/JCC-150003.

Dintwa, K. F., Letamo, G. & Navaneetham, K. (2019) Measuring social vulnerability to natural hazards at the district level in Botswana, *Journal of Disaster Risk Studies*, **11** (1), 447. https://doi.org/10.4102/jamba.v11i1.447.

Eakin, H. & Bojorquez-Tapia, L. A. (2008) Insights into the composition of household vulnerability from multicriteria decision analysis, *Global Environmental Change*, **18** (1), 112–127. doi:10.1016/j.gloenvcha.2007.09.001.

Eckstein, D., Hutfils, M. L. & Winges, M. (2020) Global Climate Risk Index 2020: Who suffers most from extreme weather events? Germanwatch.

Flato, G. M., Marotzke, J., Abiodun, B. J., Allen, M. R., Catriona, J., Stocker, F., Qin, D., Plattner, G.-K., Tignor, M., Allen, S. K., Boschung, J., Nauels, A., Xia, Y., Bex, V. & Midgley, P. M. (2013) Evaluation of climate models. In: *Climate Change 2013: The Physical Science Basis. Contribution of Working Group I to the Fifth Assessment Report of the Intergovernmental Panel on Climate Change*. Cambridge University Press, pp. 741–866.

Freitas, M. A. S. (2005) Um sistema de suporte à decisão para o monitoramento de secas meteorológicas em regiões semiáridas, *Revista de Tecnologia*, **19** (Suppl), 84–95.

Giorgi, F. & Mearns, L. O. (1999) Introduction to special section: regional climate modeling revisited, *Journal of Geophysical Research: Atmospheres*, **104** (D6), 6335–6352. doi:10.1029/98JD02072.

Govindasamy, B., Caldeira, K. & Thomson, A. M. (2003) High-resolution simulations of global climate, part 2: effects of increased greenhouse gases, *Climate Dynamics*, **21** (3), 391–404. https://doi.org/10.1007/s00382-003-0352-6.

Hahn, M., Riederer, A. & Foster, S. (2009) The livelihood vulnerability index: a pragmatic approach to assessing risks from climate variability and change – a case study in Mozambique, *Global Environmental Change*, **19**, 74–88. doi:10.1016/j.gloenvcha.2008.11.002.

Hasan, K., Rahman, M. & Kayes, A. N. (2025c) Comprehensive assessment of local climate change adaptation with provision of sustainable adaptation plan in south-west coastal region of Bangladesh: a study on Dacope Upazila, Khulna, *Progress in Disaster Science*, **26**, 100425. https://doi.org/10.1016/j.pdisas.2025.100425.

Hijmans, R. J., Cameron, S. E., Parra, J. L., Jones, P. G. & Jarvis, A. (2005) Very high-resolution interpolated climate surfaces for global land areas, *International Journal of Climatology*, **25** (15), 1965–1978. doi:10.1002/joc.1276.

Holand, I. S., Lujala, P. & Rod, J. K. (2011) Social vulnerability assessment for Norway: a quantitative approach, *Norwegian Journal of Geography*, **65** (1), 1–17. https://doi.org/10.1080/00291951.2010.550167.

Hossain, M. S., Hein, L., Rip, F. I. & Dearing, J. A. (2013) Integrating ecosystem services and climate change responses in coastal wetlands development plans for Bangladesh, *Mitigation and Adaptation Strategies for Global Change*, **20** (2), 241–261. https://doi.org/10.1007/s11027-013-9489-4.

Huq, S. & Ayers, J. (2007) Critical climate change impacts and the case for adaptation in Bangladesh, *Climate and Development*, **2** (2), 134–145.

Ido (2025) How rain and humidity are connected | Smart Fog. Smart Fog. Available at: https://www.smartfog.com/how-rain-and-humidity-connected/.

Ikart, E. M. (2019) Survey questionnaire survey pretesting method: an evaluation of survey questionnaire via expert reviews technique, *Asian Journal of Social Science Studies*, **4** (2), 1. https://doi.org/10.20849/ajsss.v4i2.565.

Importance of feature scaling (n.d.) Scikit-learn. Available at: https://scikit-learn.org/stable/auto_examples/preprocessing/plot_scaling_importance.html.

IPCC (2014) *Climate Change 2014: Impacts, Adaptation, and Vulnerability*. Cambridge, UK: Cambridge University Press.

IPCC (2021) Sixth Assessment Report. Intergovernmental Panel on Climate Change.

Islam, F. a. S. (2025) Impact of climate change and sea level rise on coastal zone of Bangladesh, *American Journal of Innovation in Science and Engineering*, **4** (1), 112–122. https://doi.org/10.54536/ajise.v4i1.4556.

Islam, M. R. & Ahmed, A. (2018) *Climate Change Adaptation: Experiences and Strategies From Coastal Bangladesh*. Cham, Switzerland: Springer.

Islam, M., Ghosh, R. C. & Faisal, M. (2019) Assessment on climate change adaptation: a study on coastal area of Khulna District in Bangladesh, *Australian Journal of Engineering and Innovative Technology*, **1** (4), 14–20. https://doi.org/10.34104/ajeit.019.14020.

Jihan, M. a. T., Popy, S., Kayes, S., Rasul, G., Maowa, A. S. & Rahman, M. M. (2025) Climate change scenario in Bangladesh: historical data analysis and future projection based on CMIP6 model, *Scientific Reports*, **15** (1), 81250. https://doi.org/10.1038/s41598-024-81250-z.

Kamal, N. & Pachauri, S. (2018) Mann-Kendall test – a novel approach for statistical trend analysis, *International Journal of Computer Trends and Technology*, **63** (1), 18–21. doi:10.14445/22312803/IJCTT-V63P104.

Kayes, M. a. N., Tabassum, T. & Khan, M. a. M. R. (2025a) Assessment of climate-induced vulnerabilities and poverty alleviation potential of dry fish industry: an ecological and socio-economic study in Cox's Bazar District, Bangladesh, *International Journal of Disaster Risk Management*, **7** (1), 461–483. https://doi.org/10.18485/ijdrm.2025.7.1.26.

Kayes, A. N. M., Pramanik, M. A. & Mim, R. S. (2025b) Assessing industrial linkage and strategic locations for sustainable economic development: a case study in North Corridor of Bangladesh, *Journal of Urban Management*. (Article in press) https://doi.org/10.1016/j.jum.2025.08.003.

Kaźmierczak, A. & Cavan, G. (2011) Surface water flooding risk to urban communities: analysis of vulnerability, hazard and exposure, *Landscape and Urban Planning*, **103**, 185–197. doi:10.1016/j.landurbplan.2011.07.008.

Khan, A. E., Ireson, A., Kovats, S., Mojumder, S. K., Khusru, A., Rahman, A. & Vineis, P. (2011) Drinking water salinity and maternal health in coastal Bangladesh: implications of climate change, *Environmental Health Perspectives*, **119** (9), 1328–1332. doi:10.1289/ehp.1002804.

Mann, H. B. (1945) Nonparametric tests against trend, *Econometrica*, **13** (3), 245. https://doi.org/10.2307/1907187.

Mattah, M. M., Mattah, P. a. D., Mensah, A., Babanawo, D., Brempong, E., Mensah, J. & Addo, K. A. (2023) Assessment of social factors that promote the vulnerability of communities to coastal hazards in the Volta estuary in Ghana, *International Journal of Disaster Risk Reduction*, **95**, 103896. https://doi.org/10.1016/j.ijdrr.2023.103896.

McFarlane, N. A., Laprise, R. & Dugas, B. (1992) The Canadian Climate Centre second-generation general circulation model and its response to greenhouse gas doubling, *Journal of Climate*, **5** (10), 1372–1383.

Mojid, M. A. (2020) Climate change-induced challenges to sustainable development in Bangladesh, *IOP Conference Series: Earth and Environmental Science*, **423** (1), 012001. https://doi.org/10.1088/1755-1315/423/1/012001.

Mondal, M. M. A., Malek, M. A., Puteh, A., Ismail, M. R., Ashrafuzzaman, M. & Naher, L. (2012) Effect of foliar application of chitosan on growth and yield in okra, *Australian Journal of Crop Science*, **6** (5), 817–823.

NASA (2023) What is climate change? NASA Global Climate Change. Available at: https://climate.nasa.gov/resources/global-warming-vs-climate-change/.

Nelson, G. C., Valin, H., Sands, R. D., Havlík, P., Ahammad, H., Deryng, D., Elliott, J., Fujimori, S., Hasegawa, T., Heyhoe, E., Kyle, P., Von Lampe, M., Lotze-Campen, H., Mason d'Croz, D., van Meijl, H., van der Mensbrugghe, D., Müller, C., Popp, A., Robertson, R., Robinson, S., Schmid, E., Schmitz, C., Tabeau, A. & Willenbockelo, D. (2014) Climate change effects on agriculture: economic responses to biophysical shocks, *Proceedings of the National Academy of Sciences of the United States of America*, **111** (9), 3274–3279. doi:10.1073/pnas.1222465110.

Nguyen, C. V., Horne, R., Fien, J. & Cheong, F. (2017) Assessment of social vulnerability to climate change at the local scale: development and application of a Social Vulnerability Index, *Climatic Change*, **143** (3–4), 355–370. https://doi.org/10.1007/s10584-017-2012-2.

Notenbaert, A., Karanja, S. N., Herrero, M., Felisberto, M. & Moyo, S. (2013) Derivation of a household-level vulnerability index for empirically testing measures of adaptive capacity and vulnerability, *Regional Environmental Change*, **13** (2), 459–454. doi:10.1007/s10113-012-0368-4.

Otto, I. M., Reckien, D., Reyer, C. P. O., Marcus, R., le Masson, V., Jones, L., Norton, A. & Serdeczny, O. (2017a) Social vulnerability to climate change: a review of concepts and evidence, *Regional Environmental Change*, **17** (6), 1651–1662. https://doi.org/10.1007/s10113-017-1105-9.

Outstandingdev (2025) Why does high humidity make the temperature seem hotter? Outstanding Heating & Cooling. Available at: https://www.outstandingair.com/blog/why-does-high-humidity-make-the-temperature-seem-hotter/.

Piya, L., Maharjan, L. K. & Niraj, J. (2012) Vulnerability of rural households to climate change and extremes: Analysis of Chepang households in the Mid-Hills of Nepal. In Proceedings of the International Association of Agricultural Economists (IAAE) Triennial Conference, Foz do Iguaçu, Brazil, 18–24.

Rahman, M. H., Islam, K. & Ahmed, A. (2013) Impact of climate change on agriculture in coastal areas of Bangladesh, *Journal of Environmental Protection*, **4** (12), 1041–1053.

Raziei, T. (2021) Revisiting the rainfall anomaly index to serve as a simplified standardized precipitation index, *Journal of Hydrology*, **602**, 126761. https://doi.org/10.1016/j.jhydrol.2021.126761.

Sen, P. K. (1968) Estimates of the regression coefficient based on Kendall's tau, *Journal of the American Statistical Association*, **63**, 1379–1389. doi:10.1080/01621459.1968.10480934.

Spielman, S. E., Tuccillo, J., Folch, D. C., Schweikert, A., Davies, R., Wood, N. & Tate, E. (2020) Evaluating social vulnerability indicators: criteria and their application to the social vulnerability index, *Natural Hazards*, **100** (1), 417–436. doi:10.1007/s11069-019-03820-z.

Tasnuva, A., Hossain, M. R., Salam, R., Islam, A. R. M. T., Patwary, M. M. & Ibrahim, S. M. (2021) Employing social vulnerability index to assess household social vulnerability of natural hazards: an evidence from southwest coastal Bangladesh, *Environment, Development and Sustainability*, **23** (7), 10223–10245. https://doi.org/10.1007/s10668-020-01054-9.

Tayyeh, H. K. & Mohammed, R. (2023) Analysis of NASA POWER reanalysis products to predict temperature and precipitation in Euphrates River basin, *Journal of Hydrology*, **619**, 129327. https://doi.org/10.1016/j.jhydrol.2023.129327.

Uddin, M. J. (2023) Climate change, vulnerabilities, and migration: insights from ecological migrants in Bangladesh, *The Journal of Environment & Development*, **33** (1), 50–74. https://doi.org/10.1177/10704965231211589.

Vincent, K. & Cull, T. (2010). 'A household social vulnerability in M for evaluating adaptation projects in developing countries', *PEGNET Conference: Policy to Foster and Sustain Equitable Development in Times of Crisis*, pp. 1–16.

Wells, J. (1997) *Composite Vulnerability Index: A Revised Report*. London: Commonwealth Secretariat.

Wilson, R. & Seatone Consulting (n.d.) Impacts of climate change on mangrove ecosystems in the coastal and marine environments of Caribbean Small Island Developing States (SIDS). In: Buckley, P., Townhill, B., Trotz, U., Nichols, K., Murray, P., Clarke-Samuels, C., Gordon, A. & Taylor, M. (eds.) *Caribbean Marine Climate Change Report Card: Science Review 2017*. pp. 61–82. Available at: https://www.crfm.int/~uwohxjxf/images/7._Mangroves_combined.pdf.

Yamane, Y. (1967) *Mathematical Formulae for Sample Size Determination*. Englewood Cliffs, NJ: Prentice-Hall.

First received 5 December 2025; accepted in revised form 15 April 2026. Available online 2 May 2026